HHS Public Access

Author manuscript

J Biomed Mater Res B Appl Biomater. Author manuscript; available in PMC 2017 April 01.

Published in final edited form as:

J Biomed Mater Res B Appl Biomater. 2016 April ; 104(3): 594–605. doi:10.1002/jbm.b.33430.

Dimensionally stable and bioactive membrane for guided bone regeneration: An *in vitro* study

Matthew J. Rowe[1,2], **Krzysztof Kamocki**[1], **Divya Pankajakshan**[1], **Ding Li**[1], **Angela Bruzzaniti**[3], **Vinoy Thomas**[4], **Steve B. Blanchard**[2], and **Marco C. Bottino**[1,*]

[1]Indiana University School of Dentistry (IUSD), Department of Restorative Dentistry, Division of Dental Biomaterials, Indianapolis, IN 46202, USA

[2]IUSD, Department of Periodontics & Allied Programs, Indianapolis, IN 46202, USA

[3]IUSD, Department of Oral Biology, Indianapolis, IN 46202, USA

[4]The University of Alabama at Birmingham (UAB), Department of Materials Science and Engineering, AL 35294, USA

Abstract

Composite fibrous electrospun membranes based on poly(DL-lactide) (PLA) and poly(ε-caprolactone) (PCL) were engineered to include borate bioactive glass (BBG) for the potential purposes of guided bone regeneration (GBR). The fibers were characterized using scanning and transmission electron microscopies, which respectively confirmed the submicron fibrous arrangement of the membranes and the successful incorporation of BBG particles. Selected mechanical properties of the membranes were evaluated using the suture pullout test. The addition of BBG at 10 wt.% led to similar stiffness, but more importantly, it led to a significantly stronger (2.37±0.51 N*mm) membrane when compared to the commercially available Epiguide® (1.06±0.24 N*mm) under hydrated conditions. Stability (shrinkage) was determined after incubation in a phosphate buffer solution from 24 h up to 9 days. The dimensional stability of the PLA:PCL-based membranes with or without BBG incorporation (10.07-16.08%) was similar to that of Epiguide® (14.28%). Cell proliferation assays demonstrated a higher rate of pre-osteoblasts proliferation on BBG-containing membranes (6.4-fold) over BBG-free membranes (4-5.8-fold) and EpiGuide® (4.5-fold), following 7 days of *in vitro* culture. Collectively, our results demonstrated the ability to synthesize, via electrospinning, stable, polymer-based submicron fibrous BBG-containing membranes capable of sustaining osteoblastic attachment and proliferation—a promising attribute in guided bone regeneration.

Introduction

Periodontitis, a chronic inflammatory disease affecting the gingiva, periodontal ligament, cementum, and underlying alveolar bone, is the leading cause of tooth loss in adults. Indeed, according to the literature, the prevalence of varying degrees of periodontitis in the United

*Corresponding author: Dr. Marco C. Bottino, Indiana University School of Dentistry, Department of Restorative Dentistry, Division of Dental Biomaterials, 1121 W. Michigan Street, Indianapolis, IN - 46202, USA, Tel: +1-317-274-3725; fax: +1-317-278-7462, mbottino@iu.edu (M.C. Bottino).

States has been estimated to affect 47.2 percent of the adult population, or 64.7 million American adults.[1]

Current treatment strategies for patients suffering from moderate-to-severe periodontal destruction often result in some form of periodontal repair; however, the goal should be the *de novo* regeneration of lost periodontal tissues, including the formation of gingiva, alveolar bone, a functionally-oriented periodontal ligament (PDL), and cementum.[1-2] Regeneration of periodontal defects has been achieved following the principle of tissue exclusion, termed guided tissue regeneration (GTR), when planned around root surfaces, or guided bone regeneration (GBR), when discussing bone defects at potential implant sites. Regenerative procedures typically involve utilization of a barrier membrane to prevent more rapidly growing epithelial tissue from migrating into the defect, allowing adequate time for the formation of PDL, cementum, and bone.[1-6]

Existing GTR/GBR membranes are often composed of synthetic polymers, which may be non-resorbable (i.e., polytetrafluoroethylene, PTFE) or resorbable (e.g., poly(lactide), PLA, and poly(ε-caprolactone), PCL). Additionally, membranes may be composed of natural polymers (e.g., collagen) combined or not combined with synthetic ones.[7-14] Even though several studies have shown that non-resorbable membranes are capable of demonstrating structural stability while providing an adequate environment for periodontal regeneration,[15] the need for a secondary surgery for membrane removal still represents a significant drawback. On the other hand, intrinsic problems with the available resorbable polymer-based synthetic membranes include poor membrane stability and bone regenerative capacity. These problems may be due to the relatively rapid degradation, shrinkage, and collapse of the membrane, which, in turn, might limit new bone formation.[14]

Electrospinning is a process by which micro/nanofibers can be formed from a viscous polymer solution exposed to an electric field.[14,16] Although widely used in tissue engineering applications,[14] biocompatible PLA electrospun meshes have displayed a high degree of shrinkage.[17-18] Importantly, Xu et al. demonstrated that combining PLA and PCL at certain ratios may control overall shrinkage,[19] which might enable its application as a GTR/GBR membrane.

In recent years, the incorporation of a wide variety of bioceramics into polymer-based scaffolds has demonstrated great potential toward the development of bioactive membranes for periodontal regeneration. Co-electrospinning hydroxyapatite with collagen and/or synthetic polymers led to improved bioactivity, greater cell adhesion, and proliferation.[20-22] Another promising material that has been used in conjunction with polymer scaffolds is bioactive glass, which has the potential to induce bone formation, osteogenic proliferation, and activation of gene expression.[23-26] Regrettably, one of the shortcomings of bioactive glass is its slow degradation. Interestingly, the partial or full replacement of silica with borate allows for greater control over the degradation rate, which is essential for bone regeneration.[27]

In the present work, borate bioactive glass (BBG) containing PLA:PCL polymer membranes was prepared via electrospinning. Morphological, chemical, and mechanical properties of

the membranes were studied in detail. In addition, membrane stability (i.e., shrinkage) over time was evaluated as a function of PCL incorporation. Lastly, preosteoblasts were cultured on the membranes to assess whether the addition of BBG could increase *in vitro* cell proliferation potentially for purposes of guided bone regeneration.

Materials and Methods

Materials

Poly(DL-lactide) (PLA, inherent viscosity 0.55–0.75 dL/g in $CHCl_3$) and poly(ε-caprolactone) (PCL, inherent viscosity 1.29 dL/g in $CHCl_3$) were purchased from Lactel Absorbable Polymers (Durect Corporation, Birmingham, AL, USA). BBG micron-sized particles with an average diameter of 1.2 μm were donated from the Mo-Sci Corporation (Cat.#1550P, Batch #101, Rolla, MO, USA). 1,1,1,3,3,3-hexafluoro-2-propanol (HFP) was used as the solvent (Sigma-Aldrich, St. Louis, MO, USA). EpiGuide®, a commercially available PLA-based resorbable periodontal membrane, was purchased from RIEMSER Pharma GmbH (Research Triangle Park, NC, USA) and used for comparative purposes.

Preparation of electrospun membranes

PLA and PCL were individually dissolved under stirring conditions in HFP to obtain 200 mg/mL and 100 mg/mL solutions, respectively. A 50:50 (v/v) polymer blend was obtained by mixing equal amounts of pure PLA and PCL solution into a fresh vial via pipetting. BBG was added to the PLA:PCL blend at two distinct concentrations (i.e., 5 and 10 wt.%, relative to the total polymer mass). A two-step method was used to obtain the BBG-containing PLA:PCL membranes. In brief, after the PLA:PCL blend preparation, BBG particles were added and sonicated (90 min) to ensure good particle dispersion.[28] Table I provides the optimized electrospinning parameters for the distinct membranes processed. The membranes were electrospun using a system consisting of a high-voltage source (ES50P-10W/DAM, Gamma High-Voltage Research Inc., Ormond Beach, FL, USA), a syringe pump (Legato 200, KD Scientific Apparatus, Holliston, MA, USA), and a grounded stainless steel collecting drum (φ = 4 cm) connected to a high-speed mechanical stirrer (BDC6015, Caframo, Georgian Bluffs, ON, Canada).[28] The distinct solutions were individually loaded into a plastic syringe fitted with a 27-gauge stainless steel needle and electrospun directly onto an aluminum foil-covered rotating mandrel. The fibers were collected at room temperature (RT). Samples were kept at RT for 2 days in a vacuum desiccator to remove any residual solvent.[28]

Membrane morphological and chemical characterizations

The fiber morphology and diameter of the resultant electrospun membranes was examined via scanning electron microscopy (SEM, JSM-5310LV, JEOL, Tokyo, Japan). Fiber morphology was imaged at 5 keV after mounting and sputter coating with Au. The mean fiber diameter (n=90) from three different images at the same magnification was calculated using ImageJ 1.40G software (National Institutes of Health, Bethesda, MD, USA).[28] Transmission electron microscopy (TEM, FEI Tecnai G20, FEI Co., Hillsboro, OR, USA) was also used to investigate the incorporation and distribution of BBG on electrospun PLA:PCL fibers. In brief, fibers composed of distinct electrospun fibrous membranes were

individually collected directly onto carbon-coated TEM grids during electrospinning. Additionally, energy-dispersive X-ray spectroscopy (EDS, EDAX/Ametek, Berwyn, PA, USA) was performed to assess the elemental composition of each electrospun membrane and the BBG used.

Mechanical suture pullout strength

Membrane tear resistance (n=4-6/group) was assessed using a suture pullout test under dry and wet conditions (i.e., PBS incubation for 24h at 37°C), since the mechanical behavior after hydration is of significant importance in predicting the *in vivo* clinical performance of the membrane.[14,28] The samples were cut (40 mm × 10 mm) and the thickness was measured (Mitutoyo Digimatic Caliper; Mitutoyo Corporation, Tokyo, Japan) at three distinct positions. The samples' measurements were averaged and entered into the testing machine (Expert 5601®, ADMET, Norwood, MA, USA) software (Quattro®).[29] The electrospun membranes were compared to EpiGuide®. A monofilament 2-0 suture (PDS II, Ethicon Z-317H) was placed 5 mm from the top edge and 5 mm from each side. The suture was affixed to the testing machine clamp but left unknotted. Testing was carried out at a crosshead speed of 1 mm/min.[30] Three distinct mechanical properties (i.e., peak load, stiffness, and energy to break) were recorded or determined from the load-position curves.

In vitro dimensional stability

The electrospun membranes (n=3), as well as EpiGuide®, were cut into squares (10 × 10 mm^2) and incubated at 37°C in PBS (2 mL) for up to 9 days. The samples were washed with distilled water and dried at RT for 24 h prior to surface area measurement. Dimensional stability (i.e., shrinkage) ratios of the electrospun membranes before and after incubation were used to obtain shrinkage rates of the samples.

In vitro osteoblast culture and cell proliferation assay

Five groups of electrospun membranes (i.e., pure PLA, pure PCL, PLA:PCL with no BBG, PLA:PCL+5 wt.%BBG, PLA:PCL+10 wt.%BBG), and EpiGuide® were studied. The fibers were electrospun onto glass cover slips (φ=12 mm) using modification of the aforementioned procedure. Samples (n=4) were exposed to UV light for 15 min and placed into wells of 24-well plates. Glass cover slips were stabilized with plastic cell crowns (CellCrown™, Scaffdex, Tampere, Finland) to prevent them from floating in culture wells. Additionally, samples were disinfected by adding 2 mL of 70% ethanol for 30 min, rinsed once with 2 mL of sterile 0.9% PBS, and soaked with 0.5 mL of minimum essential medium (MEM) supplemented with 10% fetal bovine serum, 1% L-glutamine, and a 1% antibiotic and formulation (penicillin G sodium, streptomycin sulfate) medium for 30 min.

Mouse-calvaria-derived pre-osteoblasts (ATCC, CRL-2593, American Type Culture Collection, Rockville, MD, USA) previously cultured in MEM were harvested and seeded at passage 15 on each of the experimental membranes at a density of 10,000 cells per well in a total volume of 300 μL of complete media. The cultures were kept at a constant temperature of 37°C, 5% CO_2 in a humidified atmosphere.[31] Replacement of the culture medium was performed every other day. Cell proliferation was assessed using the PMS-MTS one solution viability kit (Promega Corporation, Madison, WI, USA) after 3, 5, and 7 days. The assay's

functionality is mostly due to the measurement of NADH+H+ production, causing reductive cleavage of tetrazolium salt to the soluble formazan.[31] A total 60 μL of the assay reagent was added to each sample containing 300 μL of MEM. Following 2 h of incubation at 37ºC and 5% CO_2 in a humidified atmosphere, 100 μL from each 24-wells plate was transferred into wells of a 96-wells plate in triplicate and absorbance was determined at 490 nm. The MC3T3-E1 cells, seeded directly onto 24-wells plates, served as a high control. As a background, optical density measured at 650 nm was used for samples, per the manufacturer's recommendations. Four samples per time point were used to determine the number of cells attached to the electrospun fibers, as well as to EpiGuide®. Two additional samples per group and per time point were included in the cell experiment to qualitatively observe the morphology of the cells via SEM. The cells cultured on glass substrates were used as a positive control.[31] Briefly, following removal of the samples from the culture medium, the samples were fixed in buffered 4% formaldehyde (Sigma) and washed with PBS to remove unbound cells. Next, the samples were dehydrated using ascending ethanol gradients (30, 50, 70, 90, and 100%) and soaked in ethanol/hexamethyldisilazane (HMDS) gradients (Sigma). Then, the membranes were incubated in 100% HMDS and allowed to airdry. Finally, the samples were mounted on aluminum stubs, sputter-coated with Au, and imaged using SEM.[29]

Statistical analyses

Kruskal-Wallis and Student-Newman-Keuls statistical analyses were performed for fiber diameter. Two-way ANOVA was used to test the effects of the group (*i.e.*, Epiguide®, PLA, PCL, PLA:PCL, PLA:PCL+5wt.%BBG, and PLA:PCL+10wt.%BBG) and hydration status (*i.e.*, dry vs. wet), and their interaction on the distinct mechanical properties were evaluated. A natural log transformation of the outcomes was used for analysis. Two-way ANOVA analyses were used for dimensional stability assessment and cell proliferation. Statistical significance was set at $p<.05$.

Results

Membrane morphological (SEM/TEM) and chemical characterizations

The mean fiber diameter of the synthesized electrospun membranes ranged from 0.09 to 1.95 μm as follows: PLA (1.25±0.12μm), PCL (0.49±0.31μm), PLA:PCL (0.92±0.13μm), PLA:PCL+5wt.%BBG (0.61±0.11μm), and PLA:PCL+10wt.%BBG (0.52±0.12μm) (Figures 1 and 2). The PLA fibers (Figure 1A) were thicker when compared to the PCL fibers (Figure 1B). The mean diameter of the PLA:PCL fibers was between that of pure PLA and pure PCL fibers (Figure 1C). The commercially available PLA membrane (i.e., EpiGuide®) demonstrated varying fiber diameters and pore sizes that were generally larger than those found in the electrospun membranes (Figure 1D). There was no significant difference in the mean diameter of 5wt.%- and 10wt.%0-BBG-incorporated PLA:PCL fibers (Figures 2C-2F). Incorporation of BBG decreased the mean fiber diameter when compared to pure PLA, PCL, and PLA:PCL fibers ($p<0.05$). BBG particles could be visualized as swollen areas, as well as crystal structures on the otherwise smooth PLA:PCL fibers (Figures 2C-2F). It is worth mentioning that a greater amount of BBG particles was

observed on the surface of the PLA:PCL+10 wt.%BBG (Figure 2E) than PLA:PCL+5 wt.%BBG fibers (Figure 2C).

Energy-dispersive X-ray spectroscopy (EDS) was used to assess the elemental composition of the electrospun membranes and the BBG micron-sized particles (Figure 3). PLA, PCL, and PLA:PCL demonstrated similar spectra-containing traces of carbon, oxygen, and fluorine. BBG particles displayed oxygen, sodium, magnesium, phosphorus, potassium, and calcium peaks. PLA:PCL+5wt.%BBG and PLA:PCL+10wt.%BBG samples both showed the characteristic polymer-related peaks in addition to those present in the BBG particles. TEM was done to further confirm the successful incorporation of BBG on PLA:PCL blended fibers. The PLA (Figure 4A), PCL (Figure 4B), and PLA:PCL (Figure 4C) fibers were smooth. On the other hand, the incorporation of BBG made the fibers apparently rougher and uneven. Similar to the SEM images, BBG particles were more on the surface of the PLA:PCL+10 wt.%BBG fibers (Figure 4E) as compared to that of the PLA:PCL+5 wt.%BBG fibers (Figure 4D).

Mechanical suture pullout strength

Under dry conditions, electrospun PLA had significantly ($p<0.05$) higher pullout strength (*i.e.*, peak load, Table II and Figure 5A) than all the other electrospun membranes and EpiGuide®. Meanwhile, the dry pullout strength of PCL, PLA:PCL, and PLA:PCL, with distinct amounts of incorporated BBG particles, were statistically similar ($p>0.05$). Notably, the PLA:PCL+10wt.%BBG membranes were significantly stronger than EpiGuide® ($p<0.05$) (Table II and Figure 5A). However, under wet conditions, the BBG-incorporated membranes presented similar strength when compared to the clinical reference (i.e., EpiGuide®). PLA:PCL electrospun membranes performed better than EpiGuide® under both dry and wet conditions. Overall, the addition of BBG particles did not improve membrane strength when compared to Epiguide®, except when BBG particles were added at 10 wt.% and tested under dry conditions.

Membranes based on the PLA:PCL blend demonstrated significantly lower stiffness values when compared to the PLA (Table II). The addition of BBG did not compromise this property, and more importantly, the obtained values were statistically similar to Epiguide®. As far as the influence of hydration is concerned, PLA:PCL+10wt.%BBG and Epiguide® revealed statistically similar stiffness values after 24 h of immersion in PBS (Table II). Lastly, concerning the energy to break, under dry conditions, the pure PLA and PLA:PCL +10wt.%BBG displayed the highest values (not statistically significant), followed by PLA:PCL, pure PCL, Epiguide®, and PLA:PCL+5wt.%BBG. After hydration, a significant decrease in the energy to break was seen for PLA:PCL+10wt.%BBG when compared to the PLA membranes but it remained significantly higher than Epiguide® (Table II and Figure 5B).

In vitro dimensional stability

Two-way ANOVA was used to test the effects of the dimensional stability (shrinkage, %) in each group, time, and their interaction (Table III). Overall, PLA demonstrated the highest dimensional variation among groups and time. PLA:PCL demonstrated the least dimensional

variation during the 24 h to 4-day period compared to those following 9 days of incubation. The addition of BBG particles led to a decrease in dimensional stability. PLA:PCL membranes behaved similarly to EpiGuide®; that is, they demonstrated an increasing shrinkage from day 1 to day 9.

Cell proliferation

Cell proliferation on PLA:PCL+10 wt.%BBG samples was significantly higher when compared to PLA, PCL, and PLA:PCL at day 5 (Table IV). No significant differences in proliferation were noted between the 5 and 10 wt.%-BBG-containing membranes at all time points. Only at day 7 did the addition of BBG particles reveal an increase in cell proliferation over that seen on EpiGuide®. Generally, cell proliferation among groups was greatest at day 7, with diminished proliferation compared to days 5 and 3, respectively. Although the addition of BBG particles did not demonstrate a significant improvement in cell proliferation at days 3 and 5, it did show a slight enhancement over EpiGuide® by day 7. SEM images (Figure 6A-D) demonstrated a fairly well spread-out positioning of the MC3T3-E1 preosteoblasts over the surface of the electrospun membranes with extensions of pseudopodia surrounding the center of the cells.

Discussion

The electrospinning technique has been employed in tissue engineering and is useful for synthesizing novel biomaterials, with favorable mechanical and biological properties that provide adequate surface architecture to promote cell attachment and proliferation.[30-36] The electrospun collagen fiber diameter has been shown to range from 100 to 500 nm.[21] In our study, the incorporation of BBG particles at a concentration of 5 and 10 wt.% to the PLA:PCL blend led to a considerable reduction in mean fiber diameter when compared to pure PLA:PCL (Figures 2C-2F), closely resembling the diameter of collagen fibers in bone tissue.[22] According to Jeong et al., possible changes in solution viscosity due to the incorporation of inorganic particles (e.g., hydroxyapatite nanoparticles) may significantly contribute to the decrease in fiber diameter.[35]

Considering that the clinical application of periodontal membranes generally requires suturing or tacking for stabilization into the specific location,[14,30] a suture pullout strength test was used to determine the membranes' resistance to tearing under tensile forces.[30] Although incorporation of a relatively high concentration of BBG (i.e., 10wt.%) led to a substantial improvement in the energy to break (i.e., the area under the load vs. displacement curve) of the PLA:PCL+10wt.%BBG electrospun membrane under dry conditions, most probably due to the reinforcing effects of the BBG particles, a significant decrease in this property was seen after immersion in PBS (37°C, 24 h). Based on the hydrophilic nature of the BBG particles, as well as the SEM findings that revealed a substantial amount of BBG particles at the membrane's surface, one can assume that the membrane experienced an increased PBS absorption/uptake. This can provide a localized plasticizing effect due to absorbed water, which is hydrogen-bonded to hydrophilic BBG surfaces at the regions of high BBG particles' density or BBG aggregates in the hydrophobic PLA:PCL fibers (formed as a result of incomplete dispersion of BBG particles), which, in turn, can affect mechanical

strength. In a previous study conducted by our group using nano-hydroxyapatite (nano-HAp)-incorporated electrospun fibrous scaffolds, we have observed a more pronounced fiber breakage, which resulted in a decrease in mechanical strength due to the surface erosion of embedded particles or as the nano-HAp content in fiber increases. One or both of these effects could be the reasons for the reported energy to break drastic drop (Table II) in the case of PLA:PCL incorporated with 10wt.%BBG in wet conditions as compared to the other groups. Notably, for the clinical success of regenerative therapy, it is paramount that a balance between stiffness and elasticity be achieved in the synthesis of novel membranes.[14,28] It is well known that membranes should be stiff enough to bear the compressive forces exerted by the overlying soft tissue and mastication,[28] until proper maturation of the blood clot builds underneath the membrane. Meanwhile, a very stiff membrane would not allow for good clinical manageability or utilization, since, often times, one has to cut and shape the membrane to adapt to the morphologically distinct periodontal defects.[14,28,37-38] Most importantly, the overall properties of the electrospun membrane incorporated with BBG at 10wt.% presented comparable or superior mechanical properties to that of a clinically available PLA-based membrane.

Considering the intended clinical application in regenerative periodontics as GTR/GBR membranes, we assessed *in vitro* their dimensional stability over time. Worth mentioning, based on the collected data, one could also consider the potential incorporation of BBG particles into the PCL membrane, as the PCL fibrous membranes showed (numerically) better dimensional stability by day 9, even though they were not statistically different from the PLA:PCL blend membrane. Taken together, the better mechanical properties displayed by the PLA:PCL blend membrane when compared to the pure PCL further supports incorporation of the BBG particles into the blend polymer system. Further studies are necessary to investigate the role of BBG particles when incorporated into the PCL membrane in terms of fiber dimension, mechanical property, dimensional stability, and cell-membrane interaction.

In recent years, numerous research groups have focused on the development of membranes for GTR/GBR applications that are capable of not only hindering epithelial tissue infiltration into the periodontal defect, but more importantly, promoting faster bone growth through the wise addition of calcium phosphates and bioactive glass particles.[14] One might possibly argue about the actual amount of BBG incorporated into the electrospun PLA:PCL fibers. It is worth mentioning that we employed a similar particle dispersion strategy to that previously reported by our group when synthesizing polymer fibers incorporated with hydroxyapatite (n-HAp) particles. According to our previous data, based on thermogravimetric (TGA) analysis, the theoretical addition of 10wt.% of HAp particles into the polymer solution led to the actual incorporation of 10.6± 2.6wt.%, indicating good dispersion of n-HAp in the fibers and overall success of the processing approach.[28] Further research should be performed to better understand the dissolution rate and overall degradation of the BBG particles used herein when incorporated into electrospun polymer fibers after long-term storage in a clinically relevant physiological environment. Nonetheless, silicate and borate-based bioactive glasses are extensively investigated for biomedical applications to enhance bone repair/regeneration. Although both are

osteoconductive, borate-based bioactive glasses degrade faster and convert to calcium phosphate at a remarkably rapid rate that bonds with the surrounding tissue.[39] Particles of borate bioglass, designated as 45S5B1, were almost completely converted to hydroxyapatite in less than 4 days when immersed in a 0.02 M K_2HPO_4 solution with a starting pH value of 7.0 at 37°C.[40,41]

In this study, cell proliferation revealed being influenced by time and the group of membranes used. While the cells are fairly well-defined for the electrospun membranes, it is more difficult to distinguish cell borders on the EpiGuide® membranes (Figure 5E). This may be due to cell in-growth along the pores, and within the pores of Epiguide®, which are visually larger than the pores of electrospun membranes. The distribution and surface-coverage of the pre-osteoblasts on electrospun membranes appear to be similar, regardless of the presence of BBG particles. Hence, there was an increased proliferation of pre-osteoblasts on the surface of BBG-incorporated membranes by day 7. Notably, borate glass particles with diameters of 212–355 μm have been shown to support the attachment, growth, and *in vitro* osteogenic differentiation of mesenchymal stem cells.[42] This increased cell proliferation might also be due to the increased surface roughness of the BBG-incorporated fibers when compared to the smooth PCL, PLA, and PLA:PCL fibers. A study by Fu et al. demonstrated that, when osteogenic MLO-A5 cells were cultured on borate bioglass scaffolds, a reduced cell viability was observed due to the high concentration of boron ions released into the media, even though these scaffolds supported soft tissue infiltration *in vivo*. Nonetheless, we did not observe any meaningful reduction in cell attachment, which might be correlated to the relatively small percentage of BBG used, which was not sufficiently high to induce cell toxicity. One should note that the scope of the cell-related work presented in this study was restricted. Future studies using these novel BBG-incorporated membranes should investigate cell-membrane compatibility using other cell types (e.g., periodontal ligament fibroblasts). Furthermore, the effects of BBG incorporation should be studied in detailed at the molecular level to clarify their role in pre-osteoblasts' cell functions and differentiation before *in vivo* testing using GTR/GBR periodontal defect models.

Polymer-based membranes (i.e., PLA, PCL, and PLA:PCL) were fabricated via electrospinning. PLA:PCL membranes were also spun after the incorporation of distinct amounts of BBG particles into the polymer solution. The addition of PCL to PLA increased initial dimensional stability up to day 4 and increased overall stability over 9 days when compared to PLA alone. The addition of BBG did not significantly improve membrane strength when compared to Epiguide®, except for the addition of BBG at 10 wt.% under dry conditions, when testing was conducted for suture pull-out strength. The addition of PCL to PLA helped to control shrinkage of the electrospun membranes. Overall, the membranes presented a random submicron fibrous structure capable of supporting mouse-calvaria-derived preosteoblastic cell growth and proliferation. BBG-containing membranes led to greater cell proliferation over BBG-free membranes and EpiGuide, following 7 days of culture.

Conclusion

Clinical applications of BBG-containing electrospun membranes are vast and would include the fabrication of membranes containing additional biologic modifiers, such as bone morphogenic proteins (BMPs). Future research would need to be implemented using *in vivo* animal model, to understand the role of the proposed membranes on bone regeneration. Taken together, our results demonstrated the ability to fabricate, via electrospinning, stable, polymer-based nanofibrous BBG-membranes capable of promoting osteoblast attachment and proliferation, a promising attribute that supports their use in periodontal regenerative therapy.

Acknowledgments

This research project was partially supported by a Delta Dental Foundation Grant. M.C.B. also acknowledges start-up funds from IUSD and funding from the NIH/NIDCR (Grant#DE023552). The authors are thankful to Dr. Tien-Min Gabriel Chu (IUSD) and Mo-Sci Corporation for its Borate Bioglass (BBG) donation and also Mr. George Eckert (IU School of Medicine) for his assistance with the statistical analyses.

References

1. Polimeni G, Xiropaidis AV, Wikesjö UM. Biology and principles of periodontal wound healing/regeneration. Periodontol 2000. 2006; 41:30–47. [PubMed: 16686925]
2. Melcher AH. On the repair potential of periodontal tissues. J Periodontol. 1976; 47:256–60. [PubMed: 775048]
3. Llambés F, Silvestre FJ, Caffesse R. Vertical guided bone regeneration with bioabsorbable barriers. J Periodontol. 2007; 78:2036–42. [PubMed: 18062126]
4. Polimeni G, Koo KT, Qahash M, Xiropaidis AV, Albandar JM, Wikesjö UM. Prognostic factors for alveolar regeneration: effect of tissue occlusion on alveolar bone regeneration with guided tissue regeneration. J Clin Periodontol. 2004; 31:730–5. [PubMed: 15312094]
5. Park SH, Wang HL. Clinical significance of incision location on guided bone regeneration: human study. J Periodontol. 2007; 78:47–51. [PubMed: 17199538]
6. Scantlebury TV. 1982-1992: a decade of technology development for guided tissue regeneration. J Periodontol. 1993; 64(11 Suppl):1129–37. [PubMed: 8295101]
7. Piattelli A, Scarano A, Russo P, Matarasso S. Evaluation of guided bone regeneration in rabbit tibia using bioresorbable and non-resorbable membranes. Biomaterials. 1996; 17:791–6. [PubMed: 8730963]
8. Felipe ME, Andrade PF, Grisi MF, Souza SL, Taba M, Palioto DB, Novaes AB. Comparison of two surgical procedures for use of the acellular dermal matrix graft in the treatment of gingival recessions: a randomized controlled clinical study. J Periodontol. 2007; 78:1209–17. [PubMed: 17608575]
9. Geurs NC, Korostoff JM, Vassilopoulos PJ, Kang TH, Jeffcoat M, Kellar R, Reddy MS. Clinical and histologic assessment of lateral alveolar ridge augmentation using a synthetic long-term bioabsorbable membrane and an allograft. J Periodontol. 2008; 79:1133–40. [PubMed: 18597594]
10. Behring J, Junker R, Walboomers XF, Chessnut B, Jansen JA. Toward guided tissue and bone regeneration: morphology, attachment, proliferation, and migration of cells cultured on collagen barrier membranes. A systematic review Odontology. 2008; 96:1–11. [PubMed: 18661198]
11. Gielkens PF, Schortinghuis J, de Jong JR, Paans AM, Ruben JL, Raghoebar GM, Stegenga B, Bos RR. The influence of barrier membranes on autologous bone grafts. J Dent Res. 2008; 87:1048–52. [PubMed: 18946013]
12. Milella E, Ramires PA, Brescia E, La Sala G, Di Paola L, Bruno V. Physicochemical, mechanical, and biological properties of commercial membranes for GTR. J Biomed Mater Res. 2001; 58:427–35. [PubMed: 11410902]

13. Kikuchi M, Koyama Y, Yamada T, Imamura Y, Okada T, Shirahama N, Akita K, Takakuda K, Tanaka J. Development of guided bone regeneration membrane composed of beta-tricalcium phosphate and poly (L-lactide-co-glycolide-co-epsilon-caprolactone) composites. Biomaterials. 2004; 25:5979–86. [PubMed: 15183612]
14. Bottino MC, Thomas V, Schmidt G, Vohra YK, Chu TM, Kowolik MJ, Janowski GM. Recent advances in the development of GTR/GBR membranes for periodontal regeneration--a materials perspective. Dent Mater. 2012; 28:703–21. [PubMed: 22592164]
15. Polimeni G, Albandar JM, Wikesjö UM. Prognostic factors for alveolar regeneration: effect of space provision. J Clin Periodontol. 2005; 32:951–4. [PubMed: 16104958]
16. Martins A, Reis RL, Neves NM. Electrospinning: processing technique for tissue engineering scaffolding. Int Rev Mater. 2008; 53:257–274.
17. Xie Z, B-D G, Deinnocentes P, Bird RC. Electrospun poly(D,L)-lactide nonwoven mats for biomedical application: Surface area shrinkage and surface entrapment. J Appl Polym Sci. 2011; 122:1219–1225.
18. Cui WZ, Yang Y, Li X, Jin Y. Evaluation of electrospun fibrous scaffolds of poly(dllactide) and poly(ethylene glycol) for skin tissue engineering. Mat Sci Eng C. 2009; 29:1869–1876.
19. Xu HC, Chang J. Fabrication of patterned PDLLA/PCL composite scaffold by electrospinning. J Appl Polym Sci. 2013; 127:1550–1554.
20. Yang F, Both SK, Yang X, Walboomers XF, Jansen JA. Development of an electrospun nano-apatite/PCL composite membrane for GTR/GBR application. Acta Biomater. 2009; 5:3295–3304. [PubMed: 19470413]
21. Thomas V, Jagani S, Johnson K, Jose MV, Dean DR, Vohra YK, Nyairo E. Electrospun bioactive nanocomposite scaffolds of polycaprolactone and nanohydroxyapatite for bone tissue engineering. J Nanosci Nanotechnol. 2006; 6:487–493. [PubMed: 16573049]
22. Thomas V, Dean DR, Vohra YK. Nanostructured biomaterials for regenerative medicine. Curr Nanosci. 2006; 2:155–177.
23. Schwarz K. A bound form of silicon in glycosaminoglycans and polyuronides. PNAS. 1973; 70:1608–1612. [PubMed: 4268099]
24. Schwarz K, Milne DB. Growth-promoting effects of silicon in rats. Nature. 1972; 239:333–334. [PubMed: 12635226]
25. Valerio P, Pereira MM, Goes AM, Leite MF. The effect of ionic products from bioactive glass dissolution on osteoblast proliferation and collagen production. Biomaterials. 2004; 25:2941–2948. [PubMed: 14967526]
26. Xynos ID, Edgar AJ, Buttery LD, Hench LL, Polak JM. Gene-expression profiling of human osteoblasts following treatment with the ionic products of Bioglass 45S5 dissolution. J Biomed Mater Res. 2001; 55:151–157. [PubMed: 11255166]
27. Huang W, Day DE, Kittiratanapiboon K, Rahaman MN. Kinetics and mechanisms of the conversion of silicate (45S5), borate, and borosilicate glasses to hydroxyapatite in dilute phosphate solutions. J Mater Sci Mater Med. 2006; 17:583–596. [PubMed: 16770542]
28. Bottino MC, Thomas V, Janowski GM. A novel spatially designed and functionally graded membrane for periodontal regeneration. Acta Biomater. 2011; 7:216–24. [PubMed: 20801241]
29. Bottino MC, Kamocki K, Yassen GH, Platt JA, Vail MM, Ehrlich Y, Spolnik KJ, Gregory RL. Bioactive nanofibrous scaffolds for regenerative endodontics. J Dent Res. 2013; 92:963–969. [PubMed: 24056225]
30. Norowski PA, Mishra S, Adatrow PC, Haggard WO, Bumgardner JD. Suture pullout strength and in vitro fibroblast and RAW 264.7 monocyte biocompatibility of genipin crosslinked nanofibrous chitosan mats for guided tissue regeneration. J Biomed Mater Res A. 2012; 100:2890–2896. [PubMed: 22696151]
31. KH PR, Pavasant P, Supaphol P. Effect of the surface topography of electrospun poly(epsilon-caprolactone)/poly(3-hydroxybuterate-co-3-hydroxyvalerate) fibrous substrates on cultured bone cell behavior. Langmuir. 2011; 27:10938–10946. [PubMed: 21790199]
32. Venugopal J, Ma LL, Yong T, Ramakrishna S. In vitro study of smooth muscle cells on polycaprolactone and collagen nanofibrous matrices. Cell Biol Int. 2005; 29:861–867. [PubMed: 16153863]

33. Nisbet DR, Forsythe JS, Shen W, Finkelstein DI, Horne MK. Review paper: a review of the cellular response on electrospun nanofibers for tissue engineering. J Biomater Appl. 2009; 24:7–29. [PubMed: 19074469]
34. Ravichandran R, Liao S, NG C, Chan CK, Raghunath M, Ramakrishna S. Effects of nanotopography on stem cell phenotypes. World J Stem Cells. 2009; 1:55–66. [PubMed: 21607108]
35. Jeong SI, Ko EK, Yum J, Jung CH, Lee YM, Shin H. Nanofibrous poly(lactic acid)/hydroxyapatite composite scaffolds for guided tissue regeneration. Macromol Biosci. 2008; 8:328–338. [PubMed: 18163376]
36. Lao L, Wang Y, Zhu Y, Zhang Y, Gao C. Poly(lactide-co-glycolide)/hydroxyapatite nanofibrous scaffolds fabricated by electrospinning for bone tissue engineering. J Mater Sci Mater Med. 2011; 22:1873–1884. [PubMed: 21681656]
37. Jovanovic SA, Nevins M. Bone formation utilizing titanium-reinforced barrier membranes. Int J Periodontics Restorative Dent. 1995; 15:56–69. [PubMed: 7591524]
38. Pirhonen EM, Pohjonen TH, Weber FE. Novel membrane for guided bone regeneration. Int J Artif Organs. 2006; 29:834–40. [PubMed: 17033990]
39. Kaur G, Pandey OP, Singh K, Homa D, Scott B, Pickrell G. A review of bioactive glasses: Their structure, properties, fabrication, and apatite formation. J Biomed Mater Res A J Biomed Mater Res Part A. 2014; 102A:254–274.
40. Huang W, Day DE, Kittiratanapiboon K, Rahaman MN. Kinetics and mechanisms of the conversion of silicate (45S5), borate, and borosilicate glasses to hydroxyapatite in dilute phosphate solutions. J Mater Sci Mater Med. 2006; 17:583–596. [PubMed: 16770542]
41. Manupriya, Thind KS, Singh K, Kumar V, Sharma G, Singh DP, Singh D. Compositional dependence of in-vitro bioactivity in sodium calcium borate glasses. Journal of Physics and Chemistry of Solids. 2009; 70:1137–1141.
42. Marion NW, Liang W, Reilly G, Day DE, Rahaman MN, Mao JJ. Borate glass supports the in vitro osteogenic differentiation of human mesenchymal stem cells. Mech Adv Mater Struct. 2005; 12:239–246.

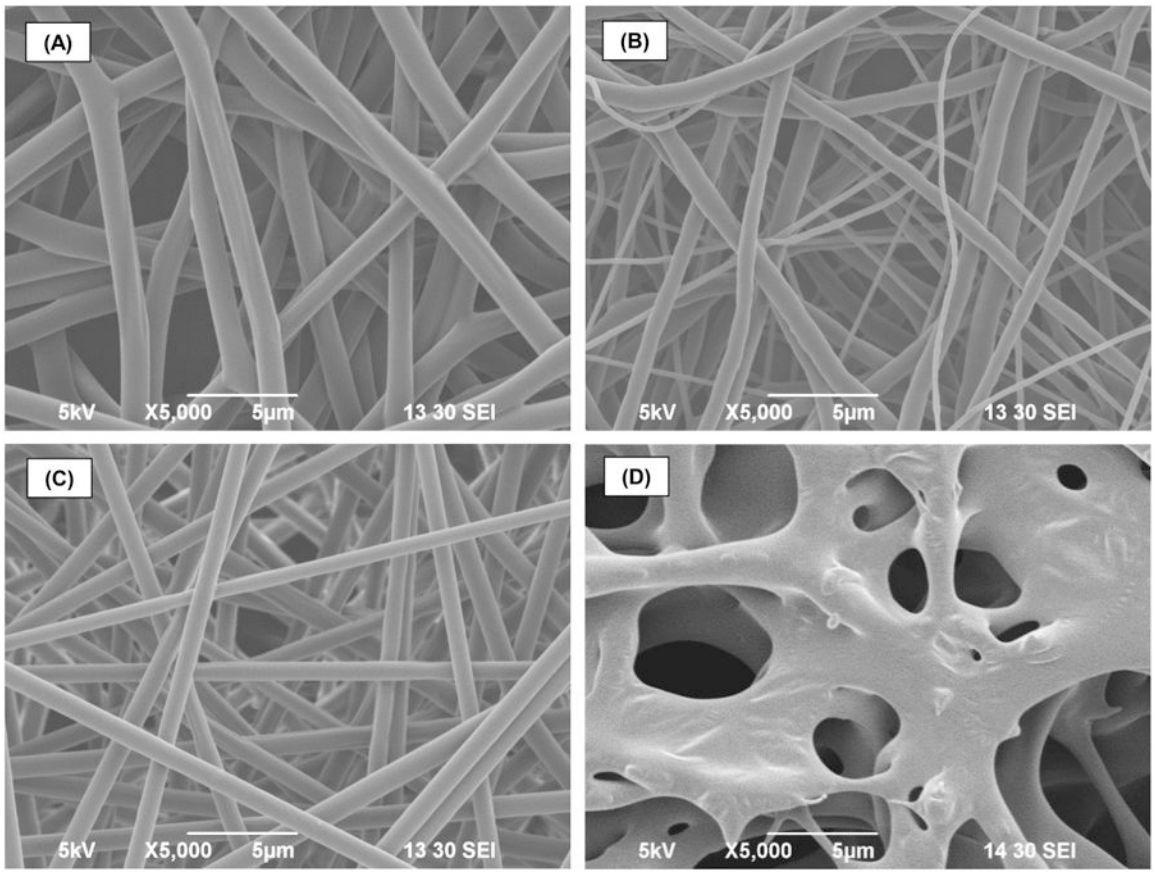

Figure 1.

Representative SEM images of the morphological structure of (A) pure PLA, (B) pure PCL, (C) PLA:PCL electrospun membranes synthesized in this study and (D) commercially available periodontal membrane, EpiGuide®.

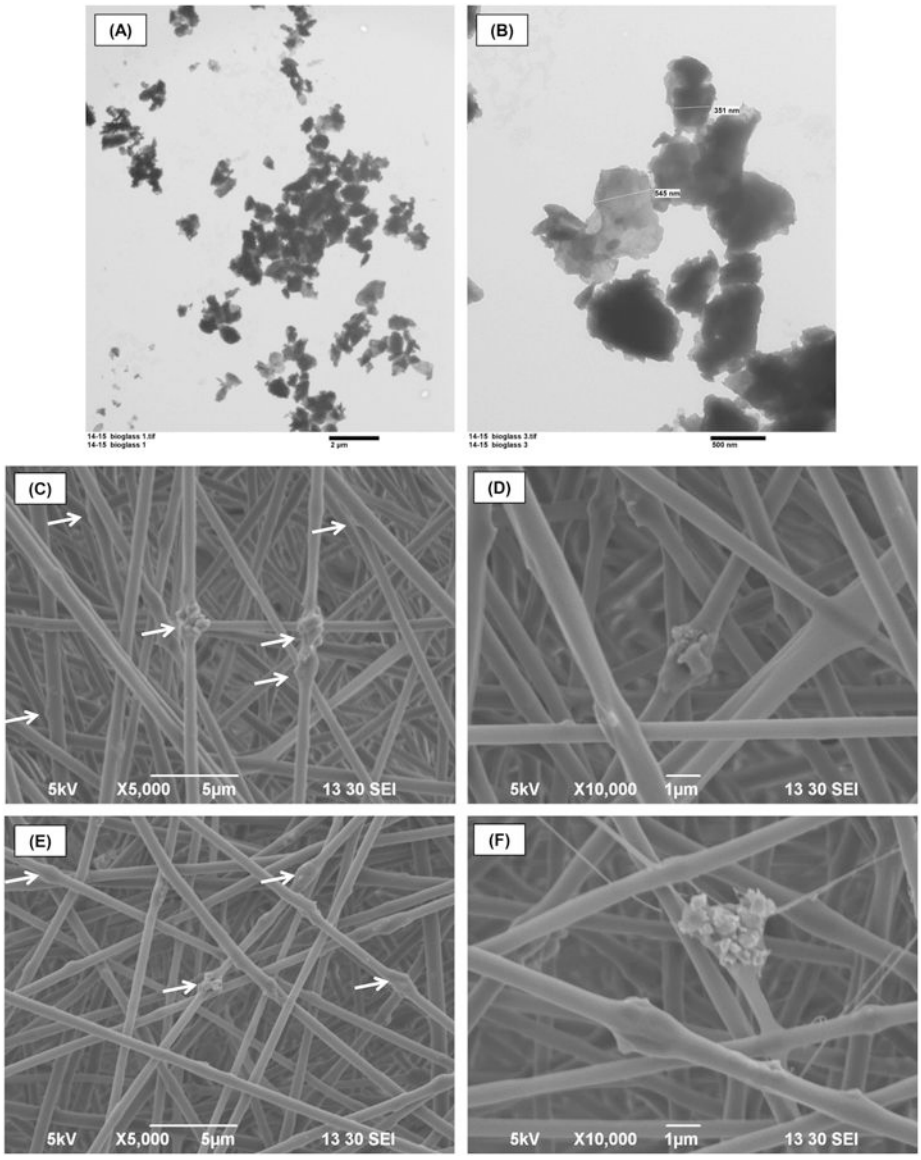

Figure 2.

(A-B) Representative TEM images of the borate-based bioglass (BBG) particles. (C-D) Representative SEM images of the PLA:PCL electrospun membranes modified with 5 wt. %BBG at 5000× (C) and 10000× (D) magnifications. (E-F) Representative SEM images of the PLA:PCL electrospun membranes modified with 10 wt.%BBG at 5000× (E) and 10000× (F) magnifications. The deposition of BBG on the PLA:PCL fibers are indicated by arrows in the lower magnification images.

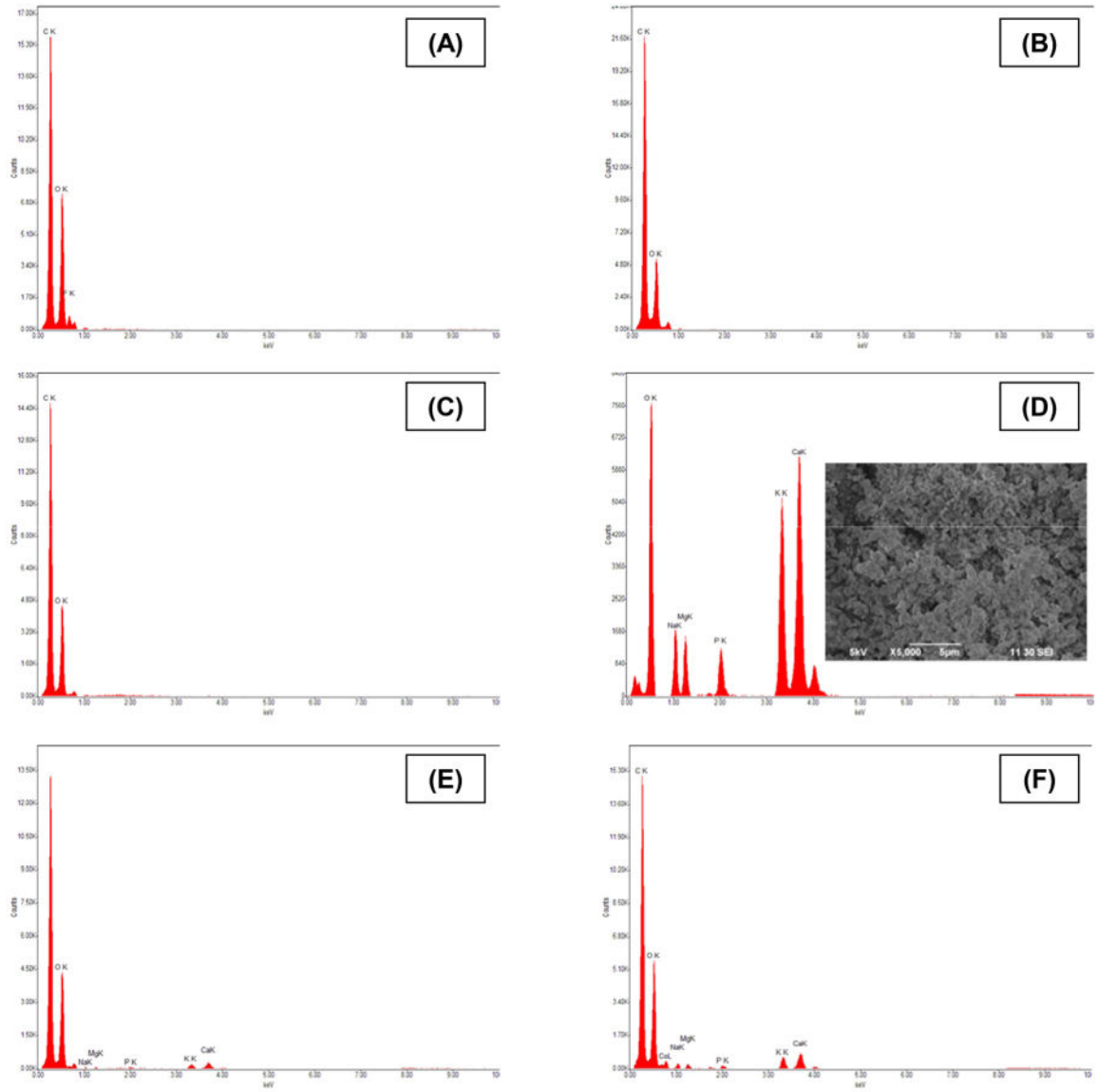

Figure 3.

EDS spectra of electrospun membranes and BBG particles. (A) PLA; (B) PCL; (C) PLA:PCL; (D) BBG particles (inset shows a representative SEM image of the BBG particles); (E) PLA:PCL+5 wt.%BBG; and (F) PLA:PCL+10 wt.%BBG.

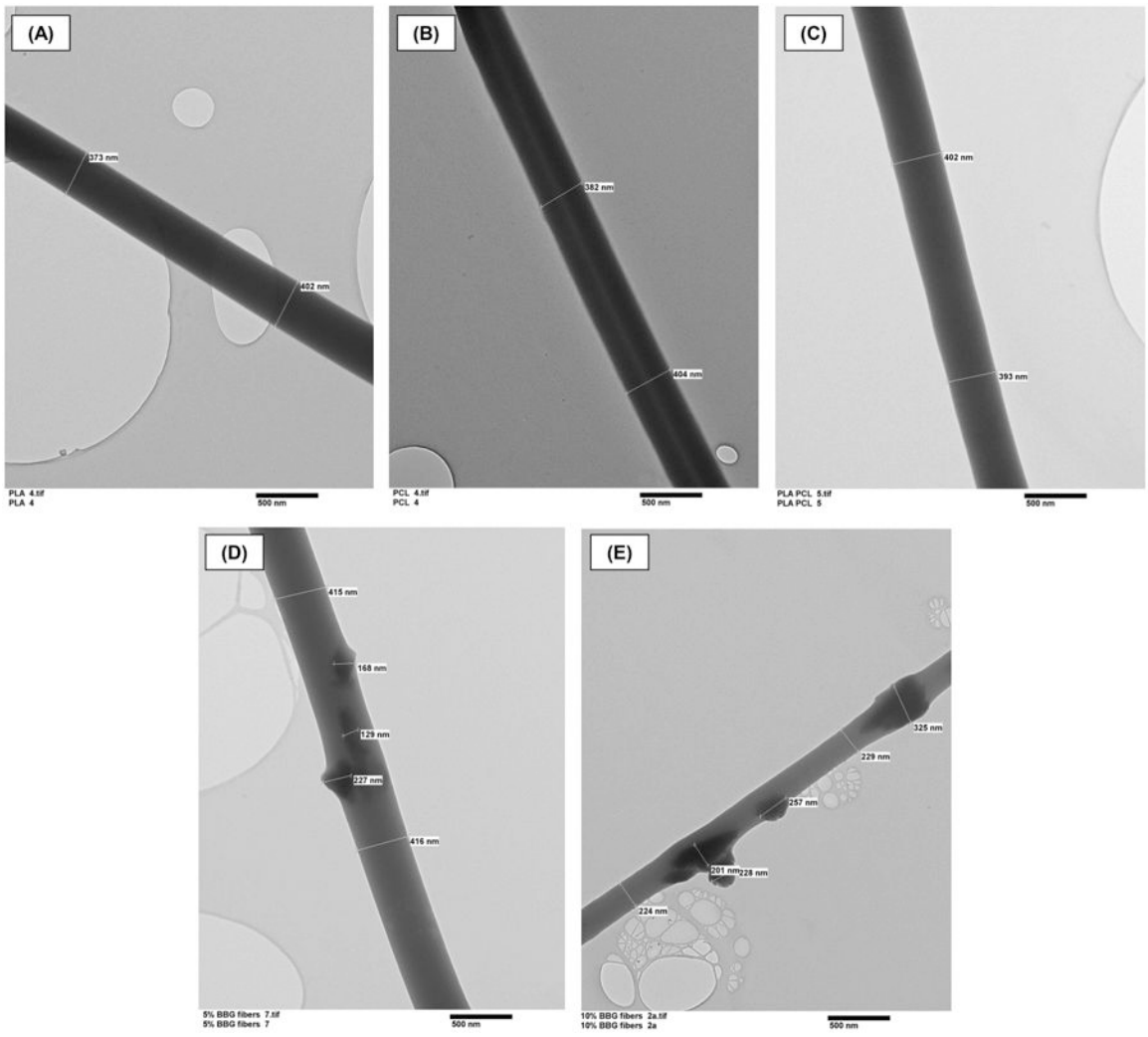

Figure 4.

Representative TEM images showing the morphology of the electrospun fibers synthesized in this study. A smooth fiber morphology can be seen in (A) pure PLA, (B) pure PCL, and (C) PLA:PCL fibers. The incorporation of BBG, regardless of the concentration (D) PLA:PCL+5wt.%BBG and (E) PLA:PCL+10 wt.%BBG led to morphologically rougher fibers. (D-E) Note the presence of BBG particles as black agglomerates along the axis of the BBG-incorporated fibers.

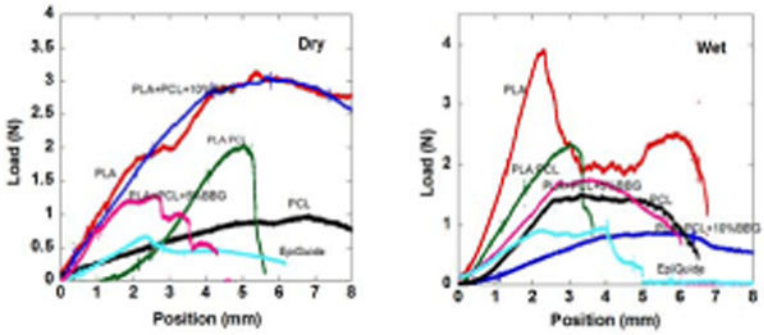

Figure 5.

Representative suture pullout strength load vs. displacement curves for all the electrospun membranes and Epiguide® under (A) dry and (B) wet conditions.

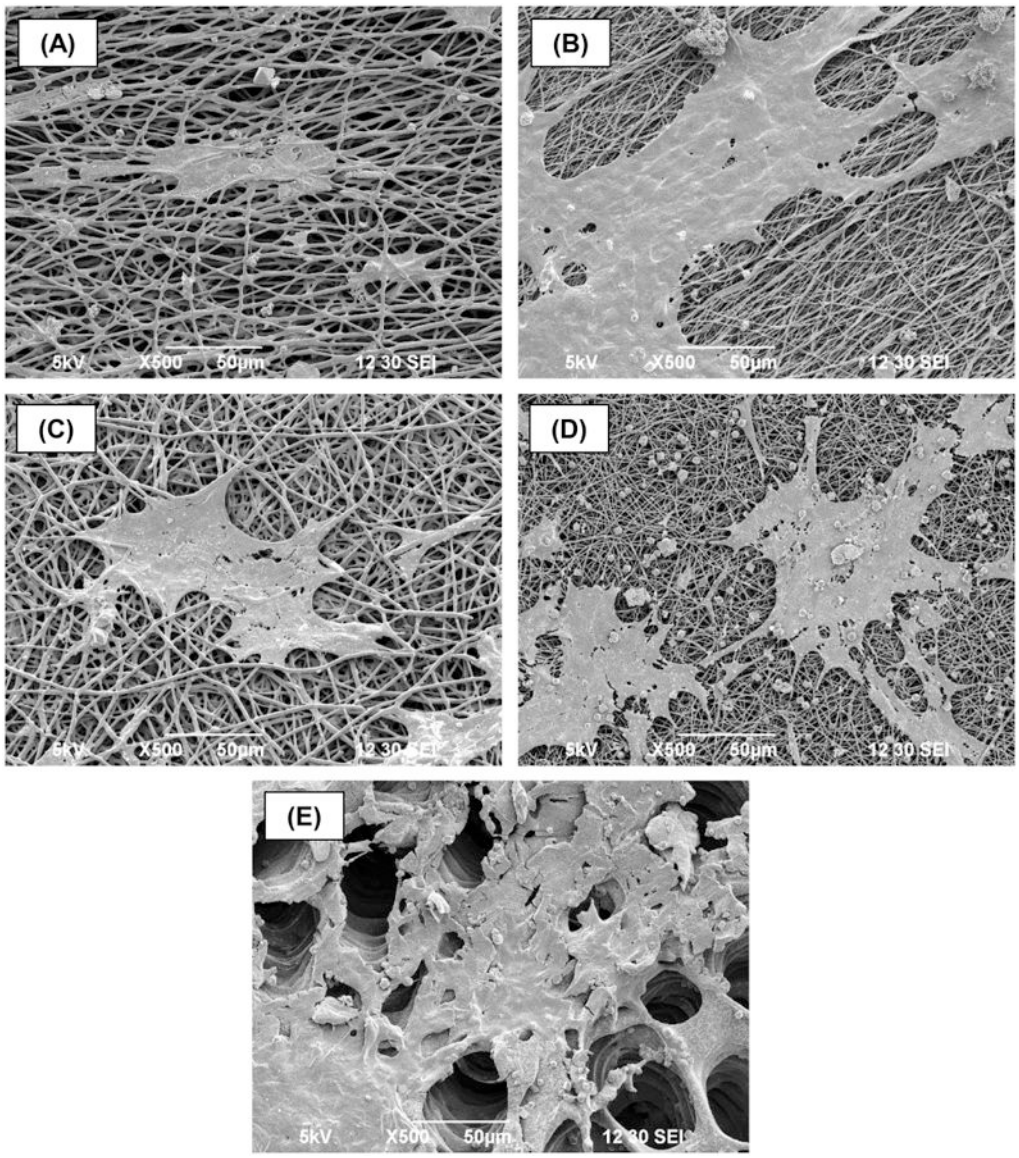

Figure 6.

Representative SEM images illustrating the MC3T3-E1 cell morphology after 7 days of culture: (a) PLA; (b) PCL; (c) PLA:PCL; (d) PLA:PCL+10 wt.%BBG; and (e) EpiGuide®.

TABLE I

Electrospinning Conditions Used for the Fabrication of Pure PLA, PCL, and Blended PLA:PCL Membranes with and without BBG Particles

Components					Electrospinning Conditions		
PLA	PCL	PLA:PCL (v/v)	BBG (wt %)	Solution Concentration	Voltage (kV)	Distance (cm)	Flow Rate (mL/h)
Pure	-	-	-	200 mg/mL (HFP)	20	18	1.0
-	Pure	-	-	100 mg/mL (HFP)	10	18	1.0
-	-	50:50	-	50:50 (v/v, HFP)	10	15	1.0
-	-	50:50	5		11	15	1.0
-	-	50:50	10				

J Biomed Mater Res B Appl Biomater. Author manuscript; available in PMC 2017 April 01.

TABLE II

Mechanical Properties of the Synthesized Electrospun Membranes and EpiGuide®

Group	Condition	Peak Load (N) Mean ± SD	Stiffness (N/mm) Mean ± SD	Energy to Break (N mm) Mean ± SD
PLA	Dry	1.80 ± 0.46[a]	5.15 ± 0.87[a]	7.20 ± 1.87[a]
PCL		0.95 ± 0.20[b]	2.00 ± 0.69[c]	3.42 ± 0.96[b]
PLA:PCL		0.91 ± 0.30[b]	2.93 ± 0.93[b]	3.88 ± 0.82[b]
PLA + PCL + 5% BBG		0.63 ± 0.15[b,c]	3.07 ± 0.41[b,c]	0.62 ± 0.16[d]
PLA + PCL + 10% BBG		1.23 ± 0.47[b,d]	2.51 ± 0.70[b,c]	9.06 ± 1.27[a]
EpiGuide®		0.55 ± 0.16[c]	2.40 ± 0.74[b,c]	1.43 ± 0.37[c]
PLA	Wet	1.78 ± 0.90[a]	7.80 ± 1.87[a]	8.21 ± 0.66[a]
PCL		0.99 ± 0.16[b]	1.99 ± 0.57[b,c]	1.96 ± 0.28[c]
PLA:PCL		0.78 ± 0.05[b]	2.64 ± 0.55[c]	5.05 ± 1.10[b]
PLA + PCL + 5% BBG		0.41 ± 0.14[c]	1.96 ± 0.63[d,c]	1.38 ± 0.39[d]
PLA + PCL + 10% BBG		0.43 ± 0.09[c]	1.40 ± 0.19[b]	2.37 ± 0.51[c]
EpiGuide®		0.44 ± 0.06[c]	1.68 ± 0.37[b]	1.06 ± 0.24[d]

Different lowercase letters in the same column represent statistical differences between groups.

TABLE III

Dimensional Stability Analysis (Shrinkage, %) After 24 h, 4 and 9 Days

Group	24 h	4 days	9 days
PLA	39.12 ± 6.29^{aB}	38.84 ± 4.03^{aB}	48.51 ± 4.83^{aA}
PCL	5.44 ± 4.0^{bA}	7.95 ± 4.51^{bA}	7.48 ± 1.66^{bA}
PLA:PCL	1.31 ± 2.37^{bA}	1.96 ± 6.40^{bA}	10.07 ± 11.39^{bA}
PLA:PCL + 5 wt % BBG	5.78 ± 2.44^{bA}	7.73 ± 5.20^{bA}	10.77 ± 5.56^{bA}
PLA:PCL+10 wt % BBG	6.23 ± 1.69^{bB}	0.81 ± 8.0^{bB}	16.08 ± 9.33^{bA}
EpiGuide®	2.35 ± 1.32^{bB}	4.66 ± 0.61^{bB}	14.28 ± 1.06^{bA}

Column corresponds to group comparisons at the specific time point (means with the same lowercase letter are not significantly different from each other). Row corresponds to time comparisons for each group (means with the same uppercase letter are not significantly different from each other).

TABLE IV
MC3T3-E1 Cell Proliferation at Days 3, 5, and 7

	Days		
	3	5	7
Group	**Mean (SD)**	**Mean (SD)**	**Mean (SD)**
PLA	16.97 ± 3.59[a,b]	18.11 ± 4.42[b,c]	105.02 ± 13.05[a,b]
PCL	14.73 ± 1.82[a,b]	14.68 ± 3.28[b,c]	60.51 ± 14.94[c]
PLA:PCL	14.24 ± 1.04[b]	12.96 ± 1.83[c]	68.17 ± 20.87[c]
PLA:PCL + 5 wt % BBG	20.32 ± 2.66[a]	20.65 ± 5.17[a,b]	128.41 ± 19.23[a]
PLA:PCL + 10 wt % BBG	19.56 ± 5.14[a,b]	28.18 ± 10.18[a]	132.6 ± 10.04[a]
EpiGuide®	17.65 ± 3.93[a,b]	20.2 ± 2.8[a,b]	89.89 ± 9.85[b,c]

Different lowercase letters in the same column represent statistical differences between group and day.